LUND UNIVERSITY

FACULTY OF SCIENCE

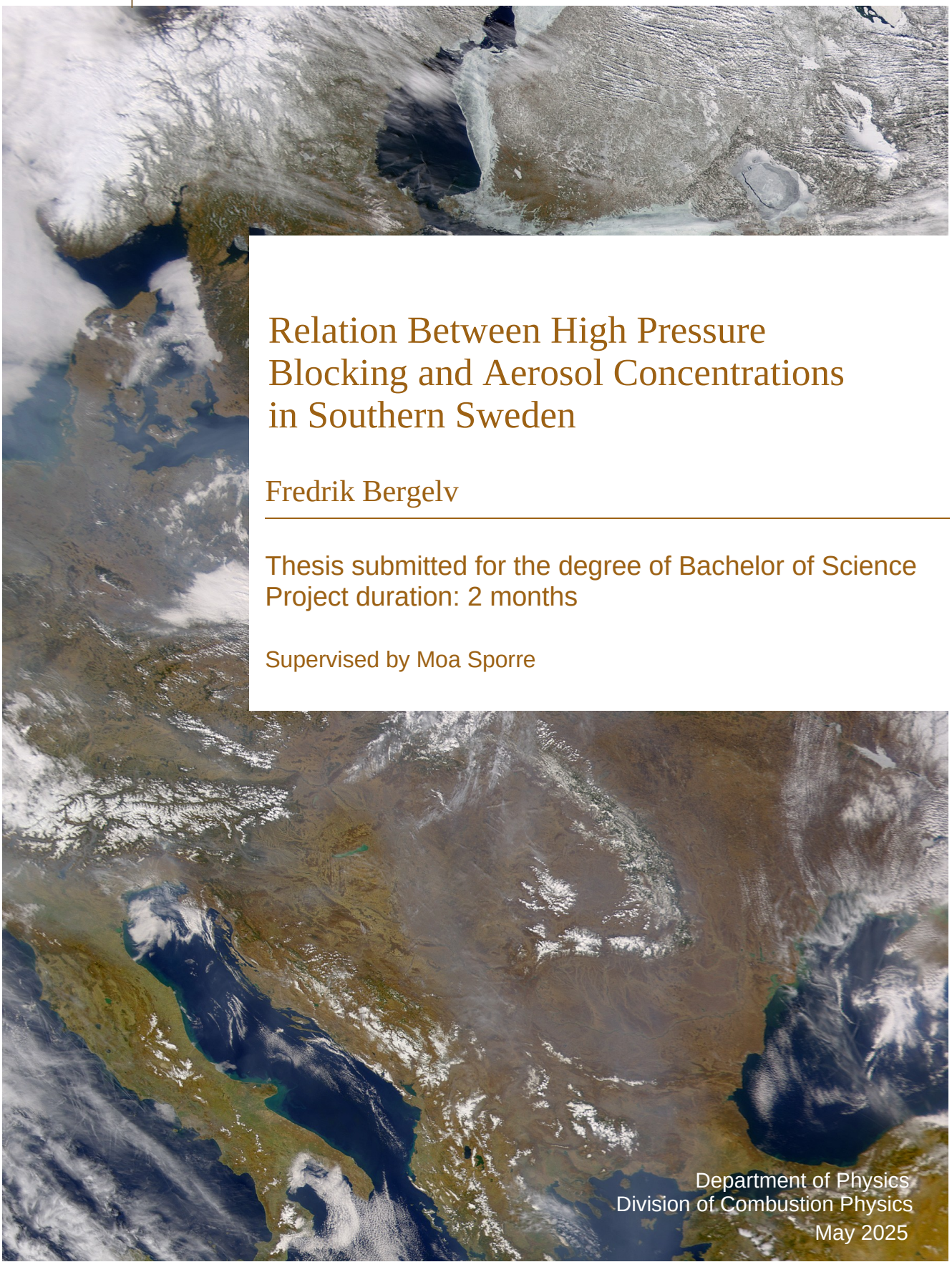

Relation Between High Pressure Blocking and Aerosol Concentrations in Southern Sweden

Fredrik Bergelv

Thesis submitted for the degree of Bachelor of Science
Project duration: 2 months

Supervised by Moa Sporre

Department of Physics
Division of Combustion Physics
May 2025

Acknowledgments

Thank you...

Cover photo taken by SeaWiFS Project, NASA, on March 28 2003 [1].

Abstract

Abstract...

Abbreviations

$PM_{2.5}$ Small particulate matter with an aerodynamic diameter less than 2.5 µm

Hfa Fennoscandian High

Sea Southeast Anticyclone

HM Central European High

Contents

1 Introduction

It is common knowledge that Earth's increasing temperature has many side effects. One such effect is the increase in frequency of extreme weather phenomena [2]. One such phenomenon, which lacks extensive research, is high-pressure blocking events. High-pressure blocking events is an anticyclone that covers an area for a prolonged period of time and often blocks other types of weather, hence the name. This results in less cloud formations and more extreme temperatures [3]. However, an anticyclone is also associated with lower air movement and wind, causing the air to remain stagnant. This can lead to an accumulation of air pollutants such as aerosols in the region [4].

To investigate the relationship between aerosols and high-pressure blocking events, one must analyse periods of high-pressure blocking and examine the concentration of aerosols during these periods. Thus, the goal of this thesis is to: identify a suitable method for detecting periods of high-pressure blocking using pressure data from SMHI; analyze these periods in relation to $PM_{2.5}$ levels from rural (Vavihill, Svalöv, Skåne County) and urban (Malmö, Skåne County) areas. Additional relevant data, such as wind direction, season, and pressure strength should be examined to gain a comprehensive understanding of high-pressure blocking events and their characteristics. The thesis will also explore the frequency of high-pressure blocking events to determine whether this weather phenomenon is becoming more common, which is particularly important if a positive correlation with aerosol levels is found. Three data sets were obtained in different intervals of time and places in order to study the relationship between thermal inversion and concentration of pollutants.

1.1 The physics behind high pressure systems

Anticyclones are more on anticyclones (Isobars, wind movement, Navier Stokes) Due to the Coriolis effect, the winds of the anticyclones rotate in a clockwise direction in the Northern Hemisphere.

Anticyclones are meteorological high-pressure systems in which air sinks toward the ground, creating high pressure [5]. This occurs due to the convergence of air from all directions at high altitudes, which forces the air to move downward. The descending air undergoes adiabatic compression, resulting in an increase in the energy of air molecules, or, in other words, a higher temperature. This rise in energy inhibits cloud formation, as warmer air can hold less moisture. The absence of clouds allows solar radiation to significantly impact the temperature during an anticyclone, leading to warmer temperatures during the day time and cooler temperatures during the night. Consequently, this leads to a large temperature difference between day and night, with summer anticyclones associated with high temperatures and winter anticyclones with low temperatures.

The Navier-Stokes equation

$$\frac{\partial \mathbf{v}}{\partial t} + (\mathbf{v} \cdot \nabla)\mathbf{v} = \mathbf{g} - \frac{\nabla p}{\rho} - 2\Omega \times \mathbf{v}, \tag{1}$$

explains the movement of the air during an anticyclone. In the Equation 1 the first term corresponds to the local acceleration of the air, the second term corresponds to the convective acceleration of the air, the third term is simply the gravitational acceleration, the fourth term describes the force from the pressure gradient and the last term describes the Coriolis force. Since we want to examine the stable solution of this equation, we can assume that the local acceleration is zero. Furthermore, since the weather system is a large scale system with the size of hundreds of kilometres, the speed is in the tens of meters per second and the Coriolis term is in the order of $0.5 \times 10^{-4}\,\mathrm{s}^{-1}$. Using this information one can observe that the size of the convection term is negligible in comparison to the Coriolis term. Lastly, one can assume the wind direction to be in the horizontal plane, making $\mathbf{v} = (v_x, v_y, 0)$ and the Coriolis term in the vertical direction as $\Omega = (0, 0, \Omega_z)$. The equation is thus simplified in the case of an anticyclone to

$$0 = -\frac{\nabla p}{\rho} - 2\Omega \times \mathbf{v}, \tag{2}$$

where the gravity is neglected since it lies in the vertical plane. Defining an anticyclone as the convergence of the pressure indicating that ∇p points inwards. One thus obtains the solution of the velocity as:

$$v_x = \frac{1}{2\rho\Omega_z}\frac{\partial p}{\partial y} \text{ and } v_y = \frac{1}{2\rho\Omega_z}\frac{\partial p}{\partial x}. \tag{3}$$

Since the derivatives are always negative since the pressure is strongest in the origin, one can observe that the rotation of the anticyclone is in the clockwise direction.

Under normal conditions the temperature of the air in the atmosphere decreases with the altitude, due to the ideal gas law. The cooling per altitude is called the environmental lapse rate and makes it possible for vertical wind movement to occur, when a slight imbalance is introduced to the system. However, during the night the air closer to the ground will lose heat due to the outgoing radiation from the Earth. This process is especially strong due to the absence of clouds during the anticyclone. This creates an inversion layer, where the air temperature increases with height for the initial height from the ground [6]. This daily cycle prohibits vertical air movement in the atmosphere.

During an anticyclone, adiabatic compression of the air occurs towards the ground. This process increases the temperature further closer to the ground. However, this downward movement of the air does not reach the ground due to the friction opposed by buildings, valleys, etc. Thus, the downward draught will spread out a few hundred meters above the ground and thus not mix with the air that lies closest to the ground. From the adiabatic compression, another inversion will be created, which makes the air closest to the ground cooler than the air a few hundred meters above ground. This process is called a subsidence inversion and will prevent air mixing between the ground level and the upper layers of the atmosphere [7].

A high-pressure blocking period refers to a prolonged anticyclone characterized by higher surface pressure covering a large area [3]. Since the blocking system extends over a vast region, the pressure gradient remains small due

to minimal fluctuations. As a result, winds tend to be calm to gentle breezes. A blocking period is typically defined as lasting between five and ten days, although no single definition exists. While the concept has been recognized in meteorology for over a century, the long-term consequences of blocking events are not yet fully understood. High-pressure blocking periods are more common in the Northern Hemisphere compared to the Southern Hemisphere. Research has indicated that the frequency of blocking periods has increased in recent years [3].

Recurring anticyclones can be classified into Hess and Brezowsky macrocirculation types, such as the Fennoscandian High (Hfa), the Southeast Anticyclone (Sea), and the Central European High (HM) [8]. These anticyclones are located at specific geographic points. Since anticyclones exhibit winds rotating clockwise around their center, the winds from Hfa, Sea, and HM tend to blow toward southern Sweden from the south and east. The transport of airborne pollutants, such as ozone, can occur via these winds [9]. Consequently, it can be hypothesized that other airborne aerosols, such as $PM_{2.5}$, should also be transported through these wind patterns.

Moving anticyclones

1.2 The origin of aerosols

The concentration of aerosols are measured through the $PM_{2.5}$, which to particulate matter with an aerodynamic diameter of 2.5 µm or less. Although these aerosols can form naturally in the atmosphere, their primary sources include solid fuel combustion for domestic heating, industrial activities, and road transportation [10]. Significant molecular contributors to the $PM_{2.5}$ levels include sulfur dioxide (SO_2) and soot (black carbon), both originating from the burning of fossil fuels. The European Union has set an annual mean limit for $PM_{2.5}$ concentrations at $25\,\mu g\,m^{-3}$. This threshold has been exceeded in several countries, including Croatia, Bosnia and Herzegovina, Italy, Poland, North Macedonia, and Türkiye [10].

Studies have demonstrated a correlation between elevated $PM_{2.5}$ concentrations and an increased risk of respiratory, cardiovascular, and cerebrovascular diseases, as well as diabetes [11]. A Danish study on on 49 564 individuals between 1993 to 2015 showed that for every $5\,\mu g\,m^{-3}$ increase in aerosol concentrations the hazard ratio increased by 1.29 [12]. Thus, for every $5\,\mu g\,m^{-3}$ increase in $PM_{2.5}$ the risk of dying from cardiovascular diseases increased by 29%. This number increased even more for people with health issues or of older age.

1.3 Aerosol concentrations during high-pressure blocking events

During an high-pressure blocking event the environmental lapse inversion, especially the subsidence inversion, close to the ground prohibits vertical air mixing during the atmospheric layers closest to the ground. If aerosols are produced at the ground level during this high-pressure blocking event, this would imply that the aerosols would not

disperse vertically, implying a higher concentration on the ground level. Thus, one would expect higher concentrations of $PM_{2.5}$ during high-pressure blocking events. Studies in China have shown that the vertical dispersion of aerosols during high-pressure blocking events are inhibited, increasing the concentration of $PM_{2.5}$ in cities [4]

Since aerosol emissions are particularly high in countries central European countries such as Poland, anticyclonic winds from Hfa, Sea, and HM are expected to increase $PM_{2.5}$ concentrations in southern Sweden [10]. These aerosols would be transported to southern Sweden via southerly to easterly winds during the anticyclone. If this occurs during a high-pressure blocking event, the aerosols may accumulate over the region while continuously being advected by southerly and easterly winds. Whether the same occurs in southern Sweden is of interest for further study.

2 Method

2.1 The data handling and devices

The relevant meteorological data was downloaded from the SMHI's website as CSV files. These files included hourly atmospheric pressure data, hourly rain data, and hourly wind data (speed and direction). Hourly aerosol data as $PM_{2.5}$, measured over one-hour intervals, was also downloaded. Since the goal of this project was to analyse aerosol concentrations in Southern Sweden during high-pressure blocking events, one urban and one rural site were selected. The locations were chosen based on their classification as rural or urban and the length of time the stations had been in operation, where more data was considered better.

2.1.1 The aerosol data and measurements

The rural measuring station with the most data was Vavihill (Svalöv, Skåne County, Sweden). This station was active from September 28, 1999, to November 15, 2017. However, due to missing data on some days, only 57 % of the period contained non missing values. Additionally, between 2017 and 2018, the Vavihill station was relocated to nearby Hallahus, where it operated from May 10, 2018, to December 31, 2022, with 93 % of the period containing non missing values. Combining these datasets resulted in a total of 5,371 days of hourly data. For an urban location in Southern Sweden, Malmö Rådhuset had the most data, with measurements recorded from June 3, 1999, to December 31, 2023. Here, 90 % of the recorded values were non missing, resulting in 8,074 days of data.

The measurement device used at Vavihill was the ambient particulate monitor TEOM 1400. This monitor continuously collects airborne particles less then 2.5 µg onto a filter and measures their mass using an oscillating microbalance technique [13]. The oscillating microbalance works by vibrating at a natural frequency, which changes as particles accumulate on the filter. Since this frequency shift is proportional to the mass of the deposited particles, their total mass can be accurately determined. The precision of the monitor was $\pm 1.5\,\mu g\,m^{-3}$. Thus, the monitor provides high precision and stable measurements. However, a key limitation is that it cannot distinguish between different types of particles, as it only measures total mass.

When the measuring station was moved to Hallahus, the measuring device was updated to the fine dust analysis system Palas FIDAS 200. This device works by an optical aerosol spectrometer which samples particles from an isokinetic inlet through a polychromatic light-scattering channel where the scattering angles and intensity were measured. [14]. This results in a high accuracy of $\pm 0.1\,\mu g\,m^{-3}$, indicating an improvement from the other device.

The monitoring station in Malmö used several measuring devices over time, in conjunction with other equipment.

Between the start of the monitoring and January 1, 2009, the TEOM 1400 monitor was used. From January 1, 2009, to December 31, 2015, the TEOM 1400, FDMS, and 8500 B or CB dryer were employed. Between January 1, 2016, and December 31, 2021, the TEOM 1405F and FDMS systems, along with the 8500 B, were in use. Finally, from January 1, 2022, the Palas FIDAS 200 monitor replaced the earlier systems. The FDMS (Filter Dynamics Measurement System) is a dynamic filter measurement system that enhances measurements by accounting for volatile and semi-volatile particles [15]. The CB dryer and 8500 B were air dryers used to prevent moisture from entering the measurement devices, ensuring accurate data by avoiding potential interference caused by water vapour.

2.1.2 The meteorological data and measurements

The choice of atmospheric pressure measurement station was Helsingborg, located 25 km from Vavihill and 49 km from Malmö. This location was chosen based on its proximity to both $PM_{2.5}$ measuring stations, the fact that neither Malmö nor Vavihill have pressure measurements from this period, and the fact that the station has been in use from August 2, 1995, with measurements taken every hour without any missing values. The period used for this station was from start until October 10, 2024. This station thus covers the entire period of the $PM_{2.5}$ data. The measurements were shown as sea-level pressure.

The barometer that has been in use for Helsingborg is a Vaisala PTB201A for the entire period, except for the periods from April 15, 2015, to April 17, 2025, and from September 19, 2004, to May 23, 2014, when a Vaisala PTB220 was used instead. Even then, the device has been serviced every year or every other year. The PTB201A digital barometer operates using a silicon capacitive absolute pressure sensor, providing stable and accurate pressure values [16]. The sensor functions by means of a flexed diaphragm inside a capacitor that bends in response to air pressure, causing a change in the capacitor's distance and thus a variation in the current. This device measures pressure in the range of 600 hPa to 1100 hPa, with an accuracy of ± 0.3 hPa. Errors in the device may arise due to environmental factors, such as exposure to condensing gases. The Vaisala PTB220 digital barometer operates in a similar manner but offers a wider measurement range of 500 hPa to 1100 hPa, with an improved accuracy of ± 0.15 hPa [17].

The relevant rain and wind data were gathered from two different stations. For Vavihill, the station at Hörby, located 35 km away, was used, and for Malmö, a weather station just 6 km away was used. The weather station at Hörby was chosen instead of Helsingborg since neither Vavihill nor Hörby are located along the coast, whereas Helsingborg is. Coastal regions experience a daily cycle of sea breezes and land breezes, which alter the wind direction. The wind and rain data from Hörby were measured from August 1, 1995, to October 1, 2020, with measurements taken every hour without any missing values. The Hörby station was temporarily relocated for a short period in 2021. The rain data from Malmö was measured from November 21, 1995, and the wind data from January 1, 1990, with both measurements ending on December 31, 2020. These stations did not lack any data.

The wind data from both Hörby and Helsingborg used the high-performance wind sensor Vaisala WAA15A for the wind speed and Vaisala WAV15A for the wind direction. These instruments were serviced and calibrated every year or every other year, and had been in use since 1995. The WAA15A anemometer measured wind speed with an accuracy of $\pm 0.17\,\mathrm{m\,s^{-1}}$, and the WAV15A wind vane measured the wind direction with an accuracy better than $\pm 3^{\circ}$ [18]. The WAA15A anemometer works by a rotating chopper disc that interrupts an infrared beam, resulting in a laser pulse proportional to the wind speed. The WAV15A wind vane uses a counterbalanced vane with an optical disc. When the vane turns, infrared LEDs detect the change in angle with the disc and phototransistors, resulting in a precise measurement of the wind angle. For rain monitoring, the Geonor T200 device had been in use for all stations since 1995. Like the wind monitor, this device had been serviced and calibrated every year or every other year. This device works by measuring precipitation with a vibrating wire sensor that detects weight changes from the water droplets[19]. The device has a measurement accuracy better than 0.1 mm. The rain measurements in Tånga was measured manually by a beaker located on a field. Thus, errors in this measurement were higher than the digital measurement devices .

The las task was to evaluate if high-pressure blocking events had become increasingly more common. For this evaluation, atmospheric pressure data from Ängelholm airport was used instead of Helsingborg due to the pressure data from Ängelholm being active from January 5, 1946, meaning it has been in service for 49 years longer than that from Helsingborg. The data period used was frm start until October 1, 2024. This station is located 44 km from Vavihill and 76 km from Malmö. However, the pressure values differed only by a mean of 0.25 hPa and a standard deviation of 0.20 hPa between December 1, 1995 to October 1. The rain data was also expanded by using daily rain data from Ängelholm since this data was gathered from January 18, 1947, to November 30, 2001. To obtain the maximum amount of the the rain data the data from Ängelholm was used together with the nearby station of Tånga. This station is located 12 km away and had been in use since December 19, 1973. For this station the period used was from start until August 31, 2024 with daily rain data.

2.2 How the high-pressure blocking evens were identified

To evaluate when there was a high-pressure blocking event for Vavihill or Malmö, the rain data and atmospheric air pressure were used. For a period to be defined as a high-pressure event, the atmospheric pressure had to be over 1014 hPa, and the rainfall had to be less than $0.5\,\mathrm{mm\,h^{-1}}$. These values were based on the fact that 1014 hPa was the mean atmospheric pressure from Helsingborg, and $0.5\,\mathrm{mm\,h^{-1}}$ was chosen since this is considered light rain. The rain-limit was set to $2\,\mathrm{mm\,d^{-1}}$ in the case where daily precipitation was used instead. This value was chosen since it corresponds to a small amount of rainfall for a day. The reason for not using a rain limit of $12\,\mathrm{mm\,d^{-1}}$ is that it corresponds to a large amount of precipitation, whereas $2\,\mathrm{mm\,d^{-1}}$ does not. The choice of $0.5\,\mathrm{mm\,h^{-1}}$ for hourly data is motivated by the fact that continuous light rain over a 24-hour period is very rare. As a result, daily precipitation levels seldom reach $12\,\mathrm{mm\,d^{-1}}$, and are more commonly around $2\,\mathrm{mm\,d^{-1}}$. For a high-pressure event to be considered a high-pressure blocking event, the criteria for a high-pressure event had to persist for at

least 120 h (5 days). This value was chosen since a 5-day limit is often considered when classifying high-pressure blocking events [3].

2.3 The data analysis

The event data was analysed by taking the mean and standard deviation of the $PM_{2.5}$ for each hour of the high-pressure blocking events, to evaluate the average progression of a aerosols over time. This was done using the Python packages `NumPy` and `pandas`. Since the high-pressure blocking events varied in length a minimum eight events was allowed when taking the mean and standard deviation on the $PM_{2.5}$ data. The mean $PM_{2.5}$ value was evaluated together with the mean $PM_{2.5}$ value in the absence of a event and the EU annual mean limit of $PM_{2.5}$. Due to the lack of $PM_{2.5}$ data during some periods, a filter was applied, stating that a period needed 85 % $PM_{2.5}$ coverage in order to be analysed.

Afterwards, the data was sorted in different ways to explore how the $PM_{2.5}$ concentration depended on different parameters. Firstly, the data was sorted into one of four wind categories: North-East (310° to 70°), South-East (70° to 190°), West (190° to 310°), and no specific direction. This was done by categorizing the data if 60 % of the wind directional data fell into one of these categories, with no wind being handled as a missing value.

Secondly, the data was sorted based on the season of the blocking. This was evaluated by taking the midpoint date of the blocking and categorizing the season by the month it occupied. December, January, and February were considered winter; June, July, and August were considered summer; and spring and autumn were the remaining months. Lastly, the data was categorized based on the strength of the high-pressure blocking, where a weak high-pressure blocking event had a mean atmospheric pressure between 1014 hPa and 1020 hPa, a medium-strength blocking event had a mean atmospheric pressure between 1020 hPa and 1025 hPa, and a strong blocking event had a mean atmospheric pressure over 1025 hPa.

The last task was to evaluate whether high-pressure blocking events had become increasingly more common. This was evaluated in two different ways: by calculating the number of days under high-pressure blocking events per year, and the number and lengths of high-pressure blocking events per year. The number of days of blocking was also sorted by the season of the blocking to provide more insight into the nature of the high-pressure blocking events.

2.4 Statistical evaluation and the Mann-Kendall test

To evaluate if the significant result was obtained, two tests were performed. The first test compared the mean and standard deviation of $PM_{2.5}$ during high-pressure blocking events with the mean and standard deviation during

periods without high-pressure blocking. Secondly, the Mann-Kendall test was performed to evaluate whether the $PM_{2.5}$ mean during high-pressure blocking events had actually increased, and if so, by how much.

The Mann-Kendall test is a non-parametric statistical test used to calculate the monotonic trend, the significant of the result and the linear trend of a dataset. This test is commonly used in climate physics due to the challenges posed by many parameters and complex distributions. The test works by calculating the difference between each time step in the dataset. The output will be a p-value below 0.05 if the test provides a significant result, meaning that the trend is unlikely to be caused by randomness. Kendall's τ-value is used to evaluate the monotonic increase of the dataset, where -1 indicates a total monotonic decrease, 1 indicates a total monotonic increase, and 0 indicates no trend. The τ-value can be summarized by the formula

$$\tau = \frac{C - D}{C + D}, \tag{4}$$

where C is the number of concordant pairs and D is the number of discordant pairs. If the result yielded a τ-value above 0.5, the result was labelled as an clear increase. Sen's slope is a method of performing linear regression on the data. The method differs from the least squares method because it uses the median to calculate the slope. This ensures that outliers, which are common in weather data, do not affect the results. Sen's slope is calculated as

$$S_i = \frac{C_{i+1} - C_i}{t_{i+1} - t_i}, \quad \text{Sen's slope} = \text{median}(S_i) \tag{5}$$

where i represents the indices, C represents the concentration of $PM_{2.5}$, and t represents time. The program used for the Mann-Kendall test was the `pymannkendall` package in Python [**?**].

3 Results

3.1 The change in aerosol concentrations

After applying the high-pressure blocking detection method to the data from Vavihill for the entire period, a total of 298 high-pressure blocking events were identified between August 1, 1995, and October 10, 2024. Of these 298 events, 155 were removed due to insufficient $PM_{2.5}$ data, as a filter requiring 85% data coverage was applied. This left 143 relevant high-pressure blocking events. For Malmö, a total of 299 high-pressure blocking events were identified between November 20, 1995, and October 1, 2024. From these, 77 events were removed due to insufficient $PM_{2.5}$ data, again applying the 85% data coverage filter. This resulted in 222 relevant high-pressure blocking events. All of the categories had a p-value approximately equal to 0. An example plot showing the periods of high-pressure blocking events can be seen in Figure 1.

Figure 1 provides insight int other categorization of high-pressure blocking events for the two different locations. One can note differences in the lengths of the events. One can also note that the event during the first of February is only observed in Malmö, but not in Vavihill. The other way around can be seen during the midway through October. Since the pressure differences between the stations only differ by a few hPa, these differences indicate a difference in precipitation, as can bee seen in the figure below.

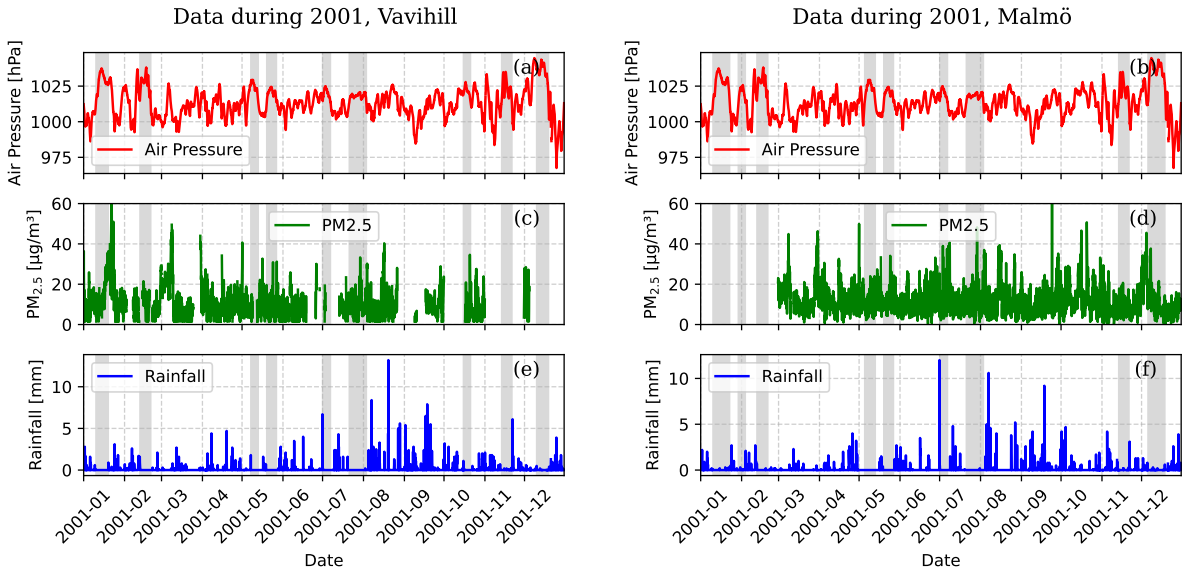

Figure 1: These example plots displays the air pressure, $PM_{2.5}$ concentrations, and rainfall during the year 2001. The periods which was indicated as periods of high-pressure blocking events are shown in gray.

The average change in $PM_{2.5}$ concentrations during periods of high-pressure blocking can be seen in Figure 2. The

data is compared with the $PM_{2.5}$ mean taken from periods without high-pressure blocking events. An increase in $PM_{2.5}$ concentrations can be seen in Malmö, while a slight increase can be observed in Vavihill. This is supported by the large τ-value in the case of Malmö (0.85), and slight lower in Vavihill (0.68). The Sen's slope values also indicate a stronger increase in Malmö 3.0×10^{-2} compared too 1.7×10^{-2} in Vavihill. After the first five days, the number of datasets decreases, which is reflected in the increase in standard deviation.

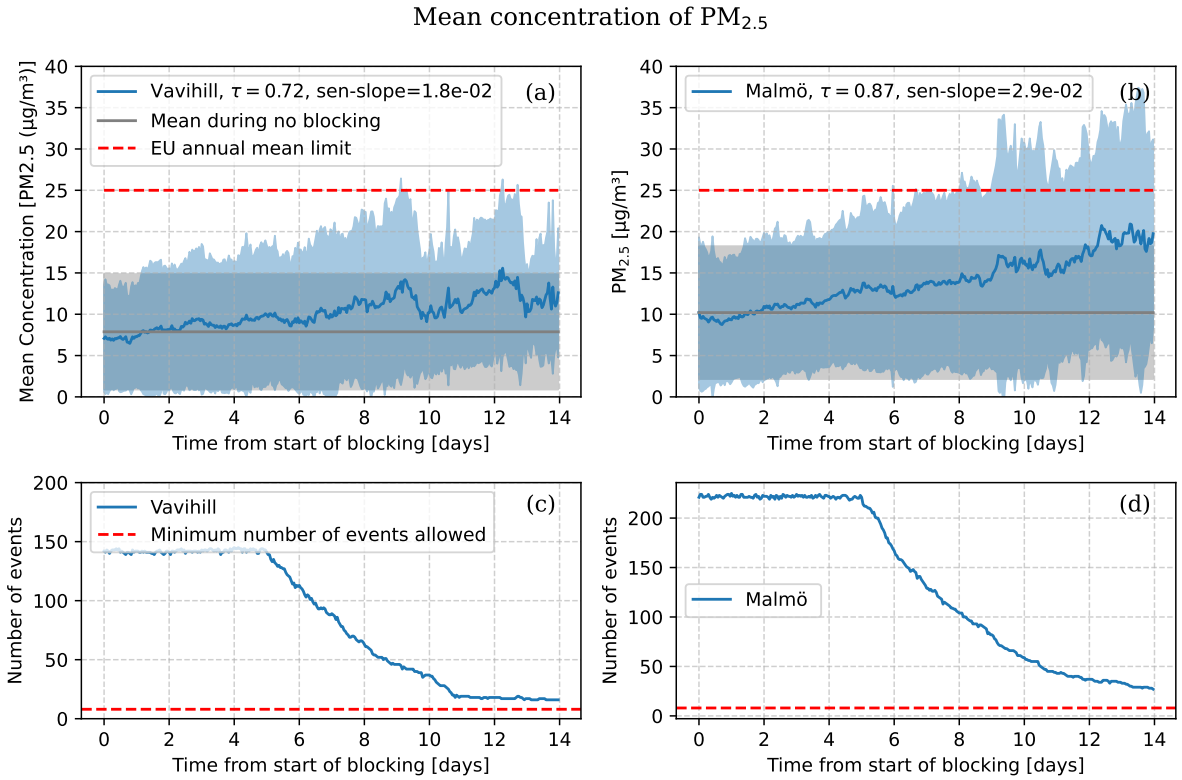

Figure 2: Comparison of mean $PM_{2.5}$ concentrations in Vavihill (a) and Malmö (b), highlighting differences between rural and urban air quality. The shaded region indicates the standard deviation of the data. The number thu number of events used in the analysis can be seen in (c) and (d).

3.2 The change in aerosol concentrations depending on wind direction

The change in $PM_{2.5}$ concentrations in Vavihill and Malmö for different wind directions can be seen in Figure 3. In the case of Vavihill, 7.0% of the winds came from the northeast (310° to 70°), 28.0% from the southeast (70° to 190°), 43.4% from the west (190° to 310°) and 43.4% from no specific direction. In the case of Malmö, 8.1% of the winds came from the northeast (310° to 70°), 23.4% from the southeast (70° to 190°), 18.5% from the west (190° to 310°) and 50.0% from no specific direction.

One can see similarities between the aerosol concentrations depending on wind directions for Vavihill and Malmö, although a larger increase can be observed Malmö. When the wind filter was applied for the northeast direction, no strong increase or high levels of $PM_{2.5}$ were detected, as supported by the τ-values being under 0.5 for both

locations. The τ-value in Vavihill for southeastern directions yielded a value of 0.33. However there is a clear increase until day nine, where the levels suddenly drop. The τ-value for the first nine days is 0.60, showing a clear increase. For the western wind direction, an increase in $PM_{2.5}$ can be seen in both locations as supported by the τ-values (0.60 for Vavihill and 0.68 för Malmö). Elevated levels can be seen in Malmö for the west direction, and especially the southeastern direction where the mean concentration exceeds the EU annual mean limit.

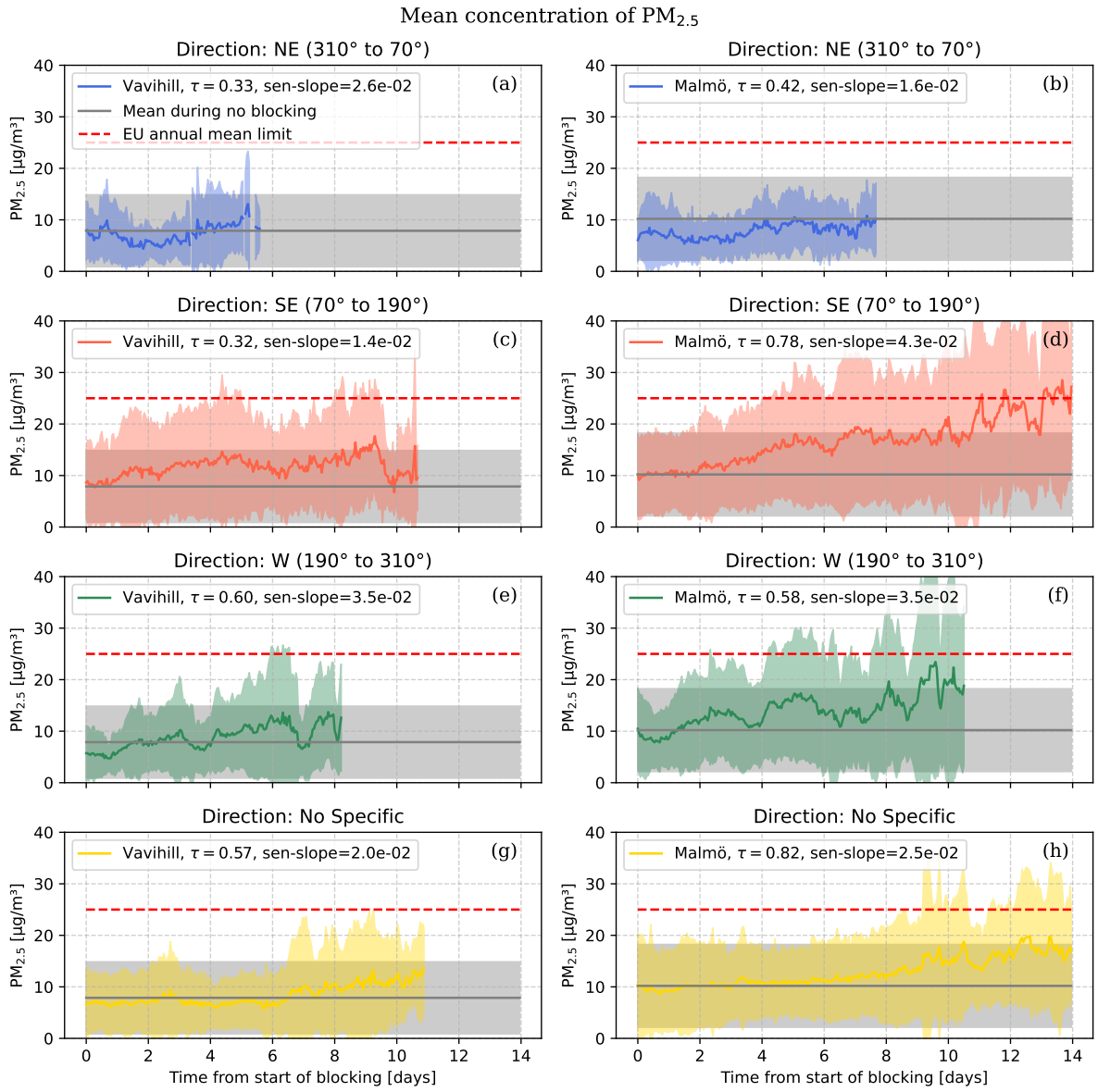

Figure 3: These plots show how $PM_{2.5}$ concentrations in Vavihill and Malmö evolve for different wind directions. A minimum number of blocking events was still put to eight, resulting in some directions having very little data.

3.3 The change in aerosol concentrations depending on season

The seasonal change in concentrations of $PM_{2.5}$ can be seen in Figure 4. From these plots, it is clear that the concentration during the summer for both Vavihill and Malmö does not indicate an increase nor high levels of

$PM_{2.5}$. In the case of Vavihill 22.9% of the blocking events occurred during the winter, 27.6% during the spring, 24.2% during the summer and 26.7% during the autumn. In the case of Malmö, 22.0% of the blocking events occurred during the winter, 32.7% during the spring, 18.0% during the summer and 27.4% during the autumn.

A slight increase can be seen in the case of spring for both locations Figure 4 (c) and (d). A larger increase can be seen during the autumn, where high levels of $PM_{2.5}$ can be observed towards the end of the period. The winter in Vavihill indicates an increase in the $PM_{2.5}$ concentrations, although the standard deviation indicates highly dispersed data. Although the τ-value during the winter in Malmö is relatively low, Sen's slope indicate a stronger increase. From the graph one can see an increase in $PM_{2.5}$ concentrations, although the levels seem to decrease towards the end of the period.

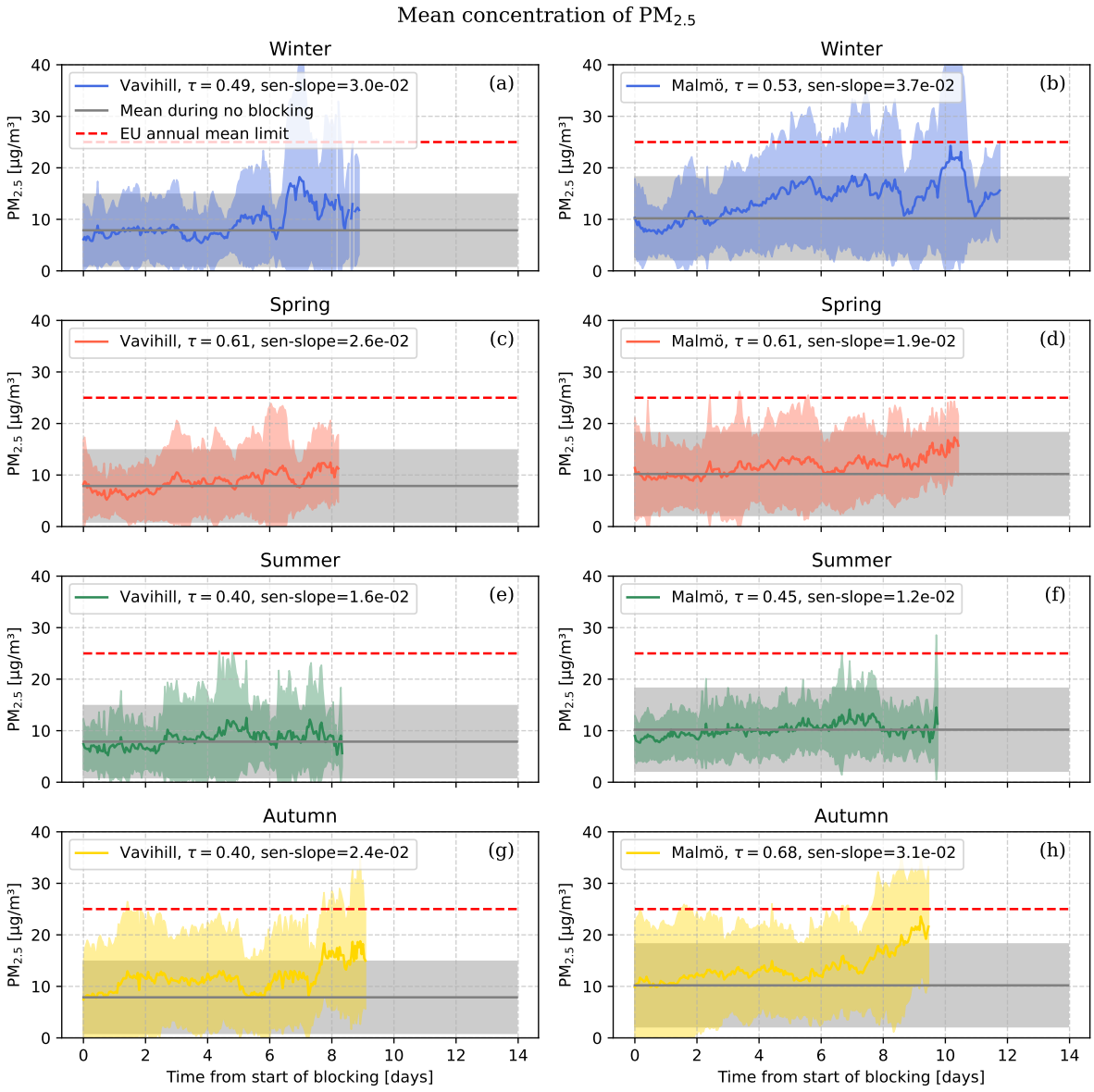

Figure 4: These plots show $PM_{2.5}$ concentrations in Vavihill and Malmö for different seasons.

3.4 The evolution of $PM_{2.5}$ depending on pressure strength

The increase in $PM_{2.5}$ concentrations depending on the strength of the high-pressure blocking event can be seen in Figure 5. In the case of Vavihill, 20.3% of the blocking events occurred with a mean pressure below 1020 hPa 45.5% occurred between 1020 and 1025 hPa and 34.3% occurred with a mean pressure over 1025hPa. In the cas of Malmö, it is important to note that 16.2% of the blocking events occurred with a mean pressure below 1020 hPa 48.2% occurred between 1020 and 1025 hPa and 35.6% occurred with a mean pressure over 1025hPa.

From the plots, we can observe similar behaviour in the two locations. In the case of weaker high-pressure blocking events no clear monotonic increase nor highly elevated levels of $PM_{2.5}$ can be seen, as seen in (a) and (b). In the case of medium strong high-pressure blocking events we see a stronger increase in the case of Vavihill τ=0.60 and weaker in Malmö from τ=0.30. However when observing both plots one can see an increase for both plots around day nine, as seen in (c) and (e). In the case of stronger high-pressure blocking events we see a strong increase in the case for Malmö, and not as clear increase in the case of Vavihill. However when viewing the plots one can observe that the levels of $PM_{2.5}$ in the case of Vavihill exceed the normal range towards the end of the period. In the case of Malmö we can see a very strong increase towards the ned, where we reach the EU annal mean limit.

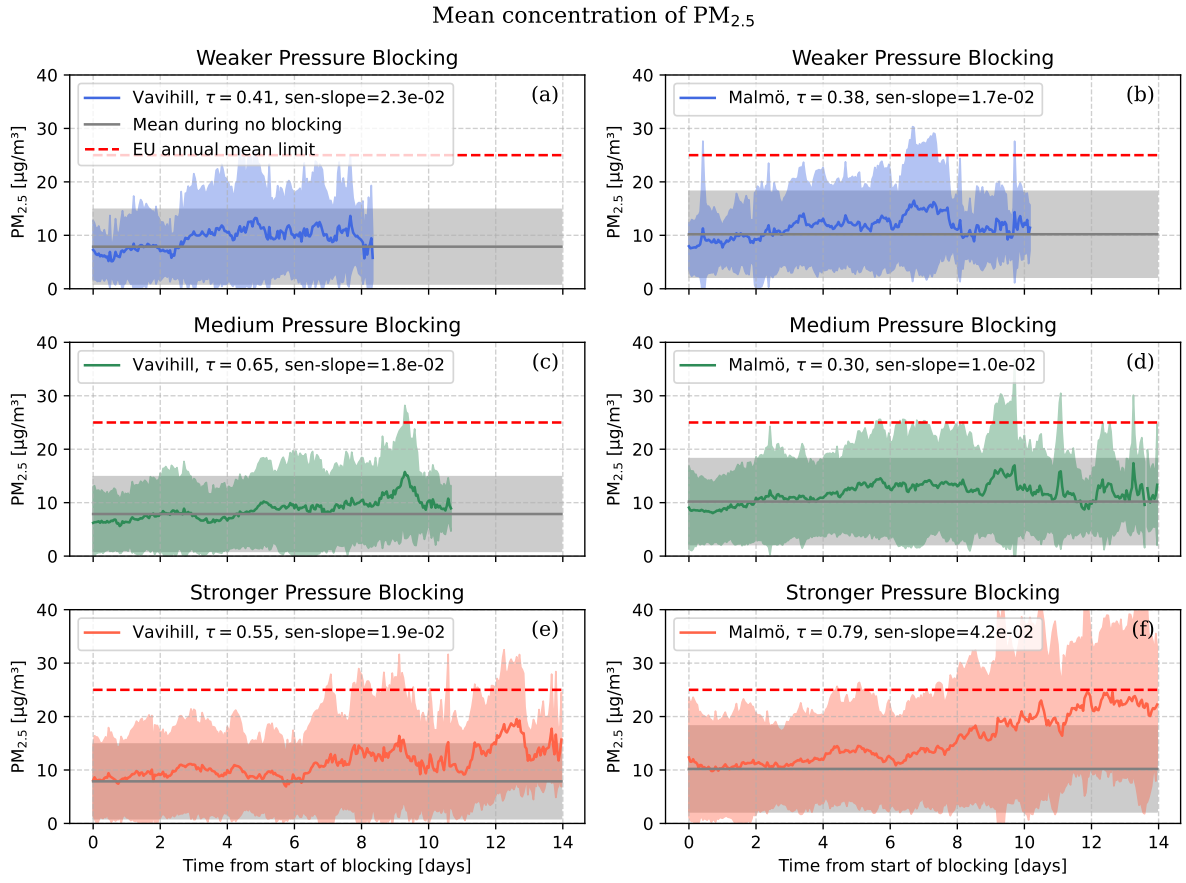

Figure 5: These plots show $PM_{2.5}$ concentrations in Vavihill and Malmö for different pressure strengths for high-pressure blocking events.

From the plots above, it is clear that the high elevations of $PM_{2.5}$ occur after nine to 13 days. This is an interesting result since this indicates that prolonged periods of high-pressure blocking events indicate an accumulative increase of $PM_{2.5}$, which can be seen in Figure 2 where we see that the combination of all the other plots resulted in a steady increase in the case of Malmö, and an increase in the case of Vavihill. The only cases where we do not see this are in the case of medium strong high-pressure blocking events. The result of weaker high-pressure blocking events is more difficult to analyse since we do not have any result for days after day nine. However, no significant increase is observed leading up to this point, indicating an absence of further increase after this point. This result points towards the fact that for stronger high-pressure blocking events, we observe an increase in the concentration of $PM_{2.5}$ after nine to thirteen days regardless of the type of high-pressure blocking event, even though different types of high-pressure blocking events may differ in the increase.

3.5 The frequency of high pressure blocking events

The last task was to determine whether high-pressure blocking events have become more common. When looking at the number of high-pressure blocking events per year, no significant change in frequency could be seen (see Figure 6). Since the highest levels of $PM_{2.5}$ occurred toward the end of the events (see Figure 2, Figure 3, Figure 4, and Figure 5), the frequency of longer high-pressure blocking events was also examined. However, no increase could be observed in any of the cases. More interestingly a small decrease can be observed from the τ-values and the Sen's slope values. However one must note that the p-values are much larger here than before, indicating towards a more random system.

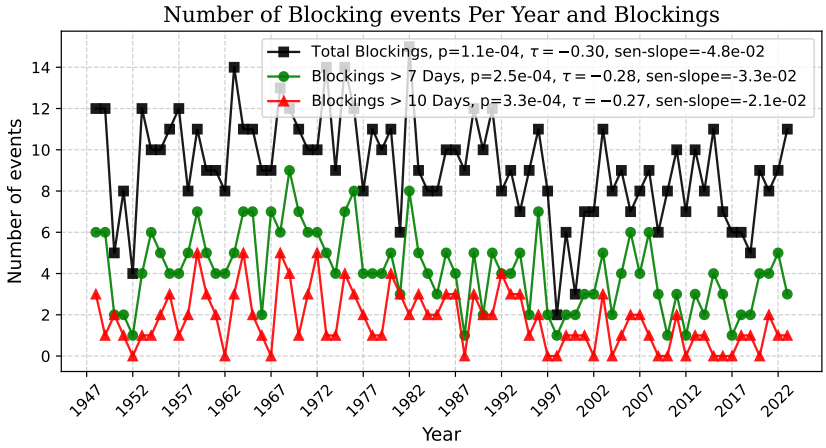

Figure 6: fig: This plots shows the change in frequency of high-pressure blocking events. The plots also indicates the change in events longer than seven and ten days.

In Figure 7, the number of days under high-pressure blocking events per year can be seen. Here, the total, seasonal, and pressure strength dependence can be observed. The reason for not including the directional dependence is that no wind data was available for this period. the number of days under high-pressure blocking events. Even here a

slight increase can be seen in most plots, especially the total blocking days per year (h).

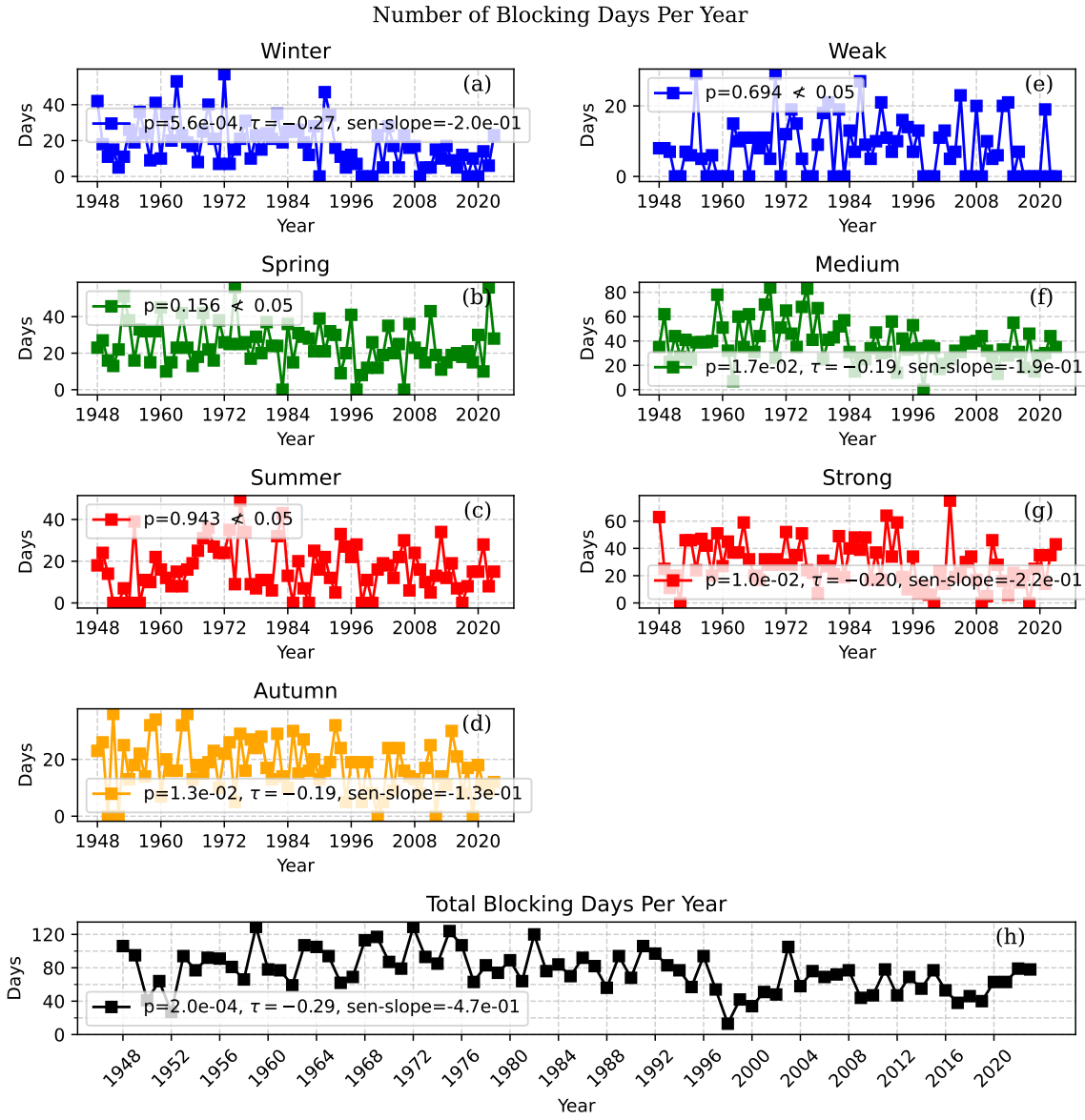

Figure 7: These plots show the change in frequency of days under high-pressure blocking events. The number of days under a high-pressure blocking event each year, during each season, and for different pressure strengths can also be seen.

4 Discussion

4.1 Analysis of periods of high aerosol concentrations

4.1.1 Why a increase is seen after 9-13 days if we have stronger high-pressure systems

The result above showed that for all high-pressure blocking events, except weaker and medium strong events, an aerosol increase was seen after nine to 13 days compared to the initial aerosol values. This result provides an important result, which is that the aerosol concentration accumulates during high-pressure blocking events. An interesting observation is that this occurs after this specific time.

4.1.2 Particle transportation versus local emissions

One important concept to discuss is whether the accumulation of aerosol is due to local emissions or particle transportation from other locations. To address this question, several observations can be made: Firstly, local emissions in urban Malmö should be much higher than those in Rural Vavihill. Secondly, if the increase is due to particle transportation, the increase should depend strongly on the wind direction.

From all the plots regarding $PM_{2.5}$ above, it is clear that the increase in Malmö is generally stronger than in Vavihill. This suggests, as predicted, that some of the increase in aerosol is due to local emissions. One could argue that this increase might be due to other factors, such as the fact that Malmö is coastal, whereas Vavihill is not, or that Malmö is located near regions with higher emissions, such as central Europe. However, this is unlikely to be the case. Firstly, the fact that Malmö is coastal would not suggest a higher aerosol increase than in Vavihill. The coastal factor may influence the overall air quality in the location, but since we are observing local changes, this factor should be accounted for. The argument is that Malmö is more closely located to central Europe, especially in the South Eastern direction. This factor may play a role in the stronger increase in Malmö than Vavihill, due to the fact that stronger high-pressure blocking events indicate slower air movement which would imply that locations closer to the locations of high emission would be impacted stronger than locations further away. However, the length scale to central Europe compared to the length scale between Vavihill and Malmö makes this factor irrelevant. Furthermore, other large urban areas such as Copenhagen are not closer to Malmö than Vavihill.

If we examine the wind dependence, we observe another interesting result. For wind direction from the northwest, there is no noticeable increase in aerosols, whereas we see a stronger increase when the wind comes from the west, and an even stronger increase from the southeastern direction. This suggests that some of the particle increase is due to particle transportation. More importantly, we observe a notable difference between the southeastern and

the northwestern directions. One could argue that this directional increase has more to do with the different types of high-pressure blocking events. However, the different types of high-pressure events such as Hfa, Sea, and HM correspond to different types of wind movement which thus means that this is the same as mentioned above.

Another argument which indicates that there is a directional dependence is comparing the data from the non-specified wind direction with the other wind directions. The non-specified wind direction showed a monotone increase for both locations; however, this increase is not as strong as the increase observed for the Western and Southeastern directions. Furthermore, the northeast direction showed a smaller increase than the non-specified direction. The non-specified direction could be the increase corresponding to the local emission, whereas the directional plots show how the local particle concentration is affected by the particles arriving with the wind. This would suggest that the wind from the northeast contains cleaner air, whereas the wind from the west and especially the southeast is exhibiting a higher aerosol concentration.

4.1.3 Urban vs. rural differences

4.1.4 Why no blockings are observed during the summer

The inversion layer only operates during the night, when no sun is present

4.1.5 Errors

What happens when large increase is cut of in mean plots?

5 Conclusion

6 Outlook

References

[1] NASA. Haze over Europe. https://earthobservatory.nasa.gov/images/11219/haze-over-europe, March 2003.

[2] John F. B. Mitchell, Jason Lowe, Richard A. Wood, and Michael Vellinga. Extreme events due to human-induced climate change. *Philosophical Transactions of the Royal Society A: Mathematical, Physical and Engineering Sciences*, 364(1845):2117–2133, 2006.

[3] Anthony R. Lupo. Atmospheric blocking events: A review. https://doi.org/10.1111/nyas.14557, December 2020.

[4] Wenyue Cai, Xiangde Xu, Xinghong Cheng, Fengying Wei, Xinfa Qiu, and Wenhui Zhu. Impact of "blocking" structure in the troposphere on the wintertime persistent heavy air pollution in northern China. *Science of The Total Environment*, 741:140325, 2020.

[5] Vlado Spiridonov and Ćurić Mladjen. Cyclones and Anticyclones | SpringerLink. https://link.springer.com/chapter/10.1007/978-3-030-52655-9_17, November 2020.

[6] Greg O'Hare, Rob Wilby, and John Sweeney and Rob Wilby. *Weather, Climate and Climate Change*. Pearson Eductaion Limited, England, 2005.

[7] E. Gramsch, D. Cáceres, P. Oyola, F. Reyes, Y. Vásquez, M. A. Rubio, and G. Sánchez. Influence of surface and subsidence thermal inversion on PM2.5 and black carbon concentration. *Atmospheric Environment*, 98:290–298, December 2014.

[8] Judit Bartholy, Rita Pongracz, and Margit Pattantyús-Ábrahám. European Cyclone Track Analysis Based on ECMWF ERA-40 Data Sets. *International Journal of Climatology*, 26(11):1517–1527, 2006.

[9] Noelia Otero, Oscar E. Jurado, Tim Butler, and Henning W. Rust. The impact of atmospheric blocking on the compounding effect of ozone pollution and temperature: A copula-based approach. *Atmospheric Chemistry and Physics*, 22(3):1905–1919, 2022.

[10] European Environment Agency. Europe's air quality status 2024. https://www.eea.europa.eu/publications/europes-air-quality-status-2024, 2024.

[11] Shubham Sharma, Mina Chandra, and Sri Harsha Kota. Health Effects Associated with PM2.5: A Systematic Review. *Current Pollution Reports*, 6(4):345–367, 2020.

[12] Ulla Arthur Hvidtfeldt, Mette Sørensen, Camilla Geels, Matthias Ketzel, Jibran Khan, Anne Tjønneland, Kim Overvad, Jørgen Brandt, and Ole Raaschou-Nielsen. Long-term residential exposure to PM2.5, PM10, black carbon, NO2, and ozone and mortality in a Danish cohort. *Environment International*, 123:265–272, February 2019.

[13] Thermo Fisher Scientific Inc. TEOM® Series 1400a Ambient Particulate (PM-10) Monitor Operating Manual, 2007.

[14] PALAS GmbH. Operating Manual: Fidas® Fine Dust Monitor System.

[15] Thermo Scientific. 8500 FDMS Filter Dynamics Measurement System, 2010.

[16] VAISALA. PTB 200 DIGITAL BAROMETERS USER'S GUIDE, February 1993.

[17] VAISALA. PTB220 Series Digital Barometers USER'S GUIDE, August 2001.

[18] VAISALA. Wind Set WA15 and WA25. https://www.vaisala.com/en/products/weather-environmental-sensors/wind-set-wa15, January 2021.

[19] GEONOR, Inc. T-200B Series All Weather Gauge. https://www.geonor.com/t-200b-all-weather-precipitation—rain-gauge, 2019.